

# Model Calibration of a Railway Vehicle

With the help of Ansys optiSlang, calibration of a numerical model of Alfa Pendular train, including the car body, bogies and passenger-seat system, was conducted based on the natural frequencies and modal configurations estimated from dynamic tests.

## / Optimization Task

When interacting with the railway track, moving trains induce vibrations that can affect the structural stability of the infrastructure, the stability of the track and of the wheel-rail contact and passengers' comfort. Complex models of the train-track coupled system are developed in order to perform an accurate analysis of the dynamic behavior. In this type of models the modeling of the vehicles is conducted based on formulations grounded on the multibody dynamics and on formulations based on the finite-element method. In formulations based on the multibody dynamics, the car body, bogies and axles of the vehicles are modeled through rigid structures connected by springs and dampers which simulate the primary and secondary suspensions. In formulations based on the finite-element method it is possible to consider the deformability of the car body, bogies and axles. The development of these models requires the knowledge of the geometrical and mechanical parameters of the vehicle's structure.

The use of models which consider the deformability of the car body of the vehicle becomes more important due to the tendency to use increasingly lighter and slender structures in the manufacture of trains to reduce weight and construction costs. It has been shown that the flexural vibration of the car body may contribute, in a large extent, to the accelerations that passengers are subjected to. The frequencies of these vibration modes range from 8.5 Hz to 13 Hz, which is significantly relevant regarding human beings' sensitivity to vibration.

This article describes the calibration of a numerical model of an Alfa Pendular train vehicle base on modal parameters. The modal parameters of the vehicle were determined based on a set of forced vibration tests that focused specifically on the car body, bogie and passenger-seat system. The calibration of the numerical model was conducted using a multistep approach involving two phases: the first phase concerned the calibration of the model of the bogie and the second phase focused on the calibration of the complete model of the vehicle. The calibration methodology involved a sensitivity analysis and an optimization. The global sensitivity analysis was based on a stochastic sampling technique and allowed the identification of the numerical parameters that most affect the modal responses and, therefore, should be included in the optimization of the model. The optimization was carried out based on an iterative procedure using a genetic algorithm. A mode pairing criterion based on the modal strain energy using the Enhanced Modal Assurance Criterion (EMAC) was used to achieve the correct pairing of the numerical and experimental vibration modes. Finally, the modal parameters of the calibrated numerical model are compared with the modal parameters of the initial numerical model.

## Numerical Modeling

The modal analysis of the BBN vehicle was performed using a three-dimensional finite element model developed in the Ansys software. The use of a finite-element formulation allows considering the influence of the deformability of the car body, bogies and axles. Figure 1 presents a perspective of the numerical model. The car body was modeled by shell-finite elements while the bogies were modeled by beam-finite elements, with the exception of the suspensions, the connecting rods and the tilting system which were modeled by spring-damper assemblies. Additionally, the passenger-seat system was modeled, in a simplified manner, by a one-DOF system composed of a mass over a spring-damper assembly. The masses of the equipment located in the under-floor of the car body and bogies were simulated through mass elements. The structure was discretised with 1082 shell elements, 1029 beam elements and 148 spring-damper assemblies. The total number of nodes is 1902, corresponding to 10,704 degrees of freedom.

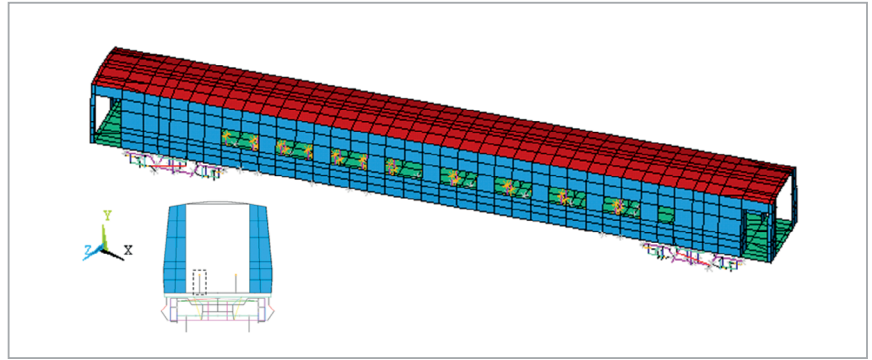


Figure 1: Numerical model of the BBN vehicle.

### Car Body

Table 1 presents the main geometric and mechanical parameters of the car body's numerical modeling, including the designation, the selected value, the unit and the bibliographic references that were used. Additionally, the characteristics of the statistical distribution of some of the parameters, later used in the calibration phase of the model are also shown. Figure 2 identifies the panels of finite elements considered in the numerical modeling of the car body in correspondence with the base, cover and side walls. In the modeling of the side walls special attention was given to the positioning of openings corresponding to windows and access doors. The finite elements that simulate the various panels have length  $l$  and constant thickness  $e$  and are constituted by elastic and orthotropic materials. The thickness of each panel was determined based on the condition that the cross-sectional area of the finite-element panel is equal to the cross-sectional area of the real panel. The inertia correction of the panels, in directions  $x$  and  $z$ , was performed using the RMI parameter (Ratio of the bending Moment of Inertia):

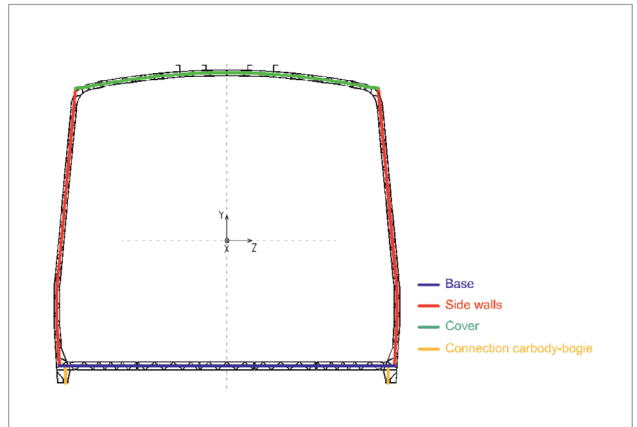


Figure 2: Finite-elements panels from the numerical modeling of the carbody.

$$RMI = \frac{I_{\text{real}}}{I_{\text{mod}}}$$

in which  $I_{\text{real}}$  is the real inertia of the panel and  $I_{\text{mod}}$  is the inertia calculated based on the thickness of the shell-finite element. The additional masses of the base, side walls and cover of the car body refer to the mass parcels of the item others under the component equipment and were uniformly distributed on the surface of the respective structural elements. The stiffness and damping parameters of the secondary suspension elements as well as their respective variation limits were estimated based on the values provided by the train's manufacturer.

Parameter	Designation	Type	Statistical distribution		Adopted value	Unit	
			Average value/ standard deviation	Limits (lower/upper)			
K <sub>S1</sub>	Stiffness of the vertical secondary suspension	Front bogie	Uniform	256.4/7.5	247/272.9	256.4	kN/m
K <sub>S2</sub>		Rear bogie					
c <sub>S</sub>	Vertical secondary suspension damping	Uniform	35/3.0	29.8/40.3	35	kN s/m	
c <sub>AL</sub>	Yaw suspsion damping	Uniform	400/34.6	340/460	400	kN s/m	
K <sub>b</sub>	Stiffness of the tilting bolster-load bolster connection rod	Uniform	20,000/8660	5000/35,000	20,000	kN/m	
ρ <sub>alum</sub>	Aluminium density	-	-/-	-/-	2700	kg/m <sup>3</sup>	
E	Modulus of deformability of aluminium	-	-/-	-/-	70	GPa	
RMI <sub>b</sub>	Corrective factor of the moment of inertia	Base	Uniform	225/101	50/400	90	-
RMI <sub>p</sub>		Side walls	Uniform	90/34.6	30/150	114	-
RMI <sub>c</sub>		Cover	Uniform	300/57.7	200/400	386	-
Δ <sub>Mb</sub>	Additional mass	Base	Uniform	70/11.5	50/90	70	%
Δ <sub>Mp</sub>		Side walls	Uniform	20/8.7	5/35	20	%
Δ <sub>Mc</sub>		Cover	Uniform	7.5/4.3	0/15	10	%
e <sub>bas</sub>	Equivalent thickness	Base	-	-/-	-/-	10.2	mm
e <sub>par</sub>		Side walls	-	-/-	-/-	10.3	mm
e <sub>cob</sub>		Cover	-	-/-	-/-	8.8	mm

Table 1: Characterization of the main parameters of the numerical model of the carbody.

## Bogie

Figure 3 (see page 4) presents a perspective of the numerical model of the bogie. The chosen colors, combined with the legend, facilitate the identification of the different elements of the bogie. The beam elements connecting the wheel sets to the axle box have zero stiffness around their axle, so as to simulate the linkage with the axle box. The support conditions imposed on the bogie, particularly on the girders and on the tilting and load bolsters, allow translational vertical movements and rotations around the x and z axes, preventing any other movements. Table 2 shows the geometrical characteristics of the sections of the various elements. The geometric characteristics are expressed in terms of the area (A) and inertias (I). Table 3 (see page next page) describes the main mechanical and geometrical parameters of the numerical model and the characteristics of the statistical distribution of certain parameters, which will be used in the model's calibration phase.

The stiffness and damping parameters of primary suspension elements and their respective variation limits were estimated based on information from the manufacturer. The additional mass of the bogie, at the girders, crossbars

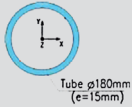
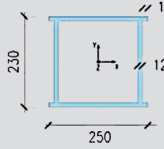
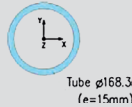
Element	Cross-section	Geometrical characteristics
Axle		A = 0.00778 m <sup>2</sup> I <sub>x</sub> = 0.267 × 10 <sup>-4</sup> m <sup>4</sup> I <sub>y</sub> = 0.267 × 10 <sup>-4</sup> m <sup>4</sup> I <sub>z</sub> = 0.534 × 10 <sup>-4</sup> m <sup>4</sup>
Girder (central zone)		A = 0.01093 m <sup>2</sup> I <sub>x</sub> = 0.857 × 10 <sup>-4</sup> m <sup>4</sup> I <sub>y</sub> = 0.887 × 10 <sup>-4</sup> m <sup>4</sup> I <sub>z</sub> = 0.121 × 10 <sup>-3</sup> m <sup>4</sup>
Crossbar		A = 0.00718 m <sup>2</sup> I <sub>x</sub> = 0.210 × 10 <sup>-4</sup> m <sup>4</sup> I <sub>y</sub> = 0.210 × 10 <sup>-4</sup> m <sup>4</sup> I <sub>z</sub> = 0.421 × 10 <sup>-4</sup> m <sup>4</sup>

Table 2: Geometric characteristics of the structural elements of the bogies.

and axles, is related to the mass of springs, dampers, connecting rods, links, reinforcement plates, axle boxes and others. These masses were linearly distributed in the different elements. In what concerns the girders the additional mass was further divided into two parcels according to their location: in the central zone, i.e. in the sections located between the crossbars and at the extremities. The wheel-rail connection was modeled by a spring element with unidirectional behavior.

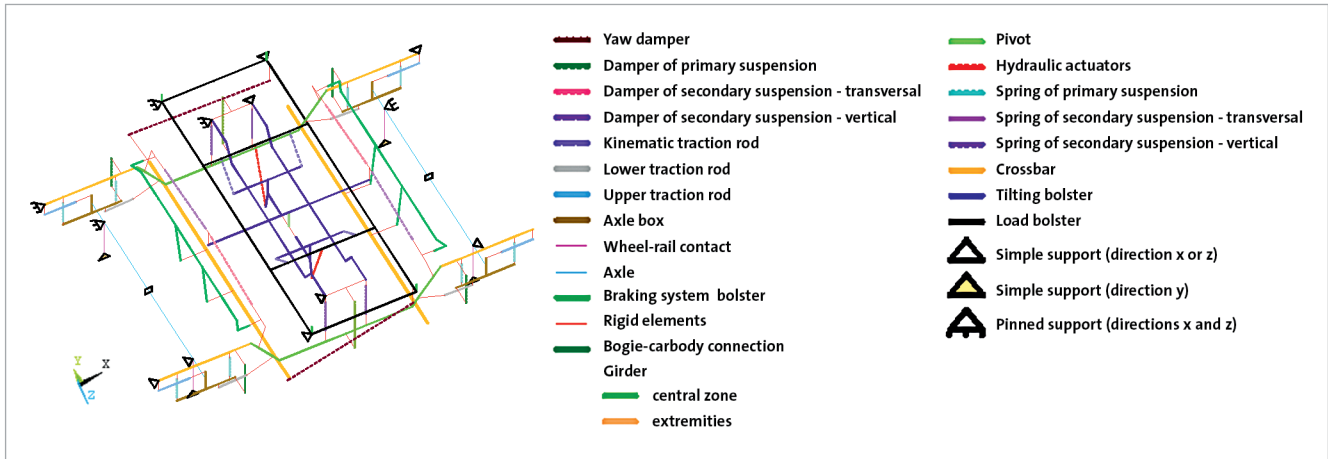


Figure 3: Numerical model of the bogie.

Parameter	Designation	Type	Statistical distribution		Adopted value	Unit
			Average value/ standard deviation	Limits (lower/upper)		
$K_p$	Stiffness of the primary suspension	Uniform	564/26.6	518/610	564	kN/m
$c_p$	Damping of the primary suspension	Uniform	18/1.6	15.3/20.7	18	kNs/m
$K_{b_{ls}}$	Stiffness of the axle box connecting rods	Upper	6.5/0.8	5.2/7.8	6.5	MN/m
$K_{b_{li}}$		Lower	25/2.9	20/30	25	MN/m
$K_{rc}$	Stiffness of the wheel-rail connection	-	-/-	-/-	$1.5674 \times 10^9$	mN/m
$\Delta M_{lc}$	Additional-mass	Girder (central area)	75/43.3	0/150	42	kg/m
$\Delta M_{le}$		Girder (extrimities)	30/17.3	0/60	38	kg/m
$\Delta M_t$		Crossbar	125/72.2	0/250	92	kg/m
$\Delta M_e$		Axles	-	-/-	-/-	271

Table 3: Characterization of the main parameters of the numerical model of the bogie.

Element	Mode	Nature of vibration mode		Damped frequency (Hz)	Undamped frequency (Hz)
Carbody	1C	Rigid body	Rolling	0.86	0.82
	2C		Bouncing	1.04	1.00
	3C		Pitching	1.42	1.33
	4C	Structural	First distortion	10.21	10.21
	5C		First bending	16.20	16.20
	6C		First torsion	15.05	15.03
Bogies	1B	Rigid body	Bouncing	8.21/8.18	6.57/6.26
	2B		Rolling	4.89/5.28	4.09/4.53
	3B		Pitching	12.10/12.04	9.50/9.41

Table 4: Numerical natural frequencies of the carbody and bogies.

### Modal parameters

Table 4 shows the damped and undamped natural frequencies of the main vibration modes of the BBN vehicle. In what concerns the bogies, for modes 1B and 2B, there are different frequency values according to the movement of the two bogies in phase and in antiphase, respectively. In the 3B mode, the different values of the frequencies are related to the isolated movements of the left and right bogies, respectively. The modal results show differences between damped and undamped natural frequencies. These differences are more notorious for the rigid body modes of the car body and bogies since these modes involve significant movements of the suspensions. In case of the bogies the differences are even more important since this additional damping is provided simultaneously by the primary and secondary suspensions. Figure 4 illustrates the modal configurations associated with rigid body modes (1C, 2C and 3C) and structural modes of distortion (4C), bending (5C) and torsion (6C) of the car body. In these modes the movements of the bogie have very low amplitude. Figure 5 shows the modal configurations, in perspective and cross-section view, of a bogie of the vehicle. Mode 1B comprises the bouncing movement of the bogie. Modes 2B and 3B comprise the rolling and pitching movements of the bogie, respectively. In these modes the car body shows very limited movements.

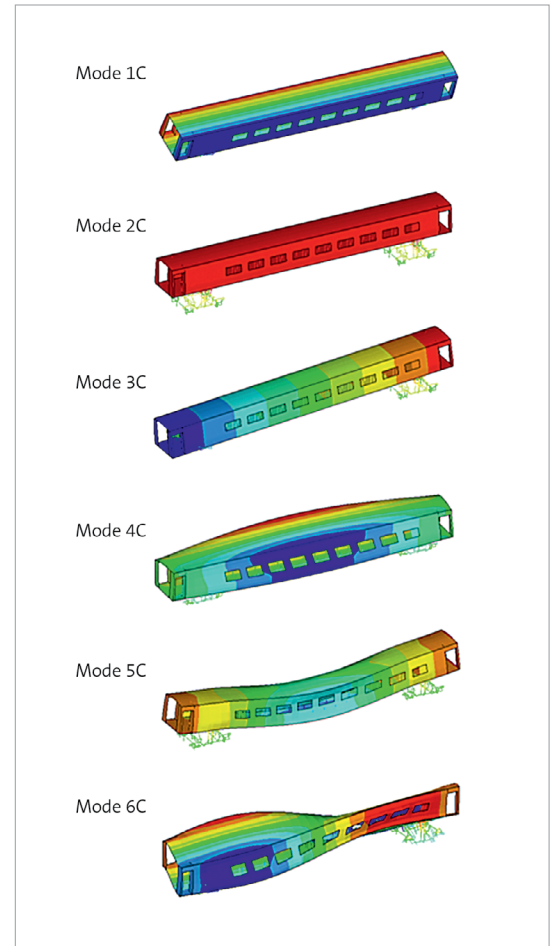


Figure 4: Numerical rigid body and structural modes of vibration of the carbody.

## Modal parameters

Table 4 shows the damped and undamped natural frequencies of the main vibration modes of the BBN vehicle. In what concerns the bogies, for modes 1B and 2B, there are different frequency values according to the movement of the two bogies in phase and in antiphase, respectively. In the 3B mode, the different values of the frequencies are related to the isolated movements of the left and right bogies, respectively. The modal results show differences between damped and undamped natural frequencies. These differences are more notorious for the rigid body modes of the car body and bogies since these modes involve significant movements of the suspensions. In case of the bogies the differences are even more important since this additional damping is provided simultaneously by the primary and secondary suspensions. Figure 4 illustrates the modal configurations associated with rigid body modes (1C, 2C and 3C) and structural modes of distortion (4C), bending (5C) and torsion (6C) of the car body. In these modes the movements of the bogie have very low amplitude. Figure 5 shows the modal configurations, in perspective and cross-section view, of a bogie of the vehicle. Mode 1B comprises the bouncing movement of the bogie. Modes 2B and 3B comprise the rolling and pitching movements of the bogie, respectively. In these modes the car body shows very limited movements.

## Calibration Methodology

The results of the conducted experimental tests of the BBN vehicle involving the dynamic tests of the car body, bogie and passenger-seat system are used to calibrate the numerical model of the vehicle. The calibration of the numerical model of the BBN vehicle was performed using an iterative method based on an optimization technique. This method consists on the resolution of an optimization problem, which consists of the minimisation of an objective function by varying a set of the preselected model parameters. The pre selection of the numerical parameters is carried out based on a global sensitivity analysis.

Figure 6 presents a flow chart illustrating the iterative method of calibration based on a genetic algorithm involving the use of three software tools: Ansys, MATLAB and Ansys optiSLang. The main aspects of the implemented calibration methodology are described in reference. The calculation of modal parameters in systems with proportional damping matrix is based on a classic modal analysis [1]. In systems with non-proportional damping matrix the same calculation is based on a state-space formulation. The mode-pairing technique aims to establish a correspondence between experimental and numerical vibration modes. This task is often complex due to alterations in the order of the numerical modes, resulting from variations on the numerical parameters which occur during the optimization process and also due to the limited number of degrees of freedom of experimental modes, which increases the number of possible correspondence between numerical and experimental modes. In this paper the correspondence between numerical and experimental modes is performed through an energetic criterion based on the modal strain energy and on the EMAC parameter. The objective function ( $f$ ) is defined based on the differences between the numerical and experimental modal parameters [1]:

$$f = a \sum_{i=1}^n \frac{|f_i^{\text{exp}} - f_i^{\text{num}}|}{f_i^{\text{exp}}} + b \sum_{i=1}^n |\text{MAC}(\varphi_i^{\text{exp}}, \varphi_i^{\text{num}}) - 1|$$

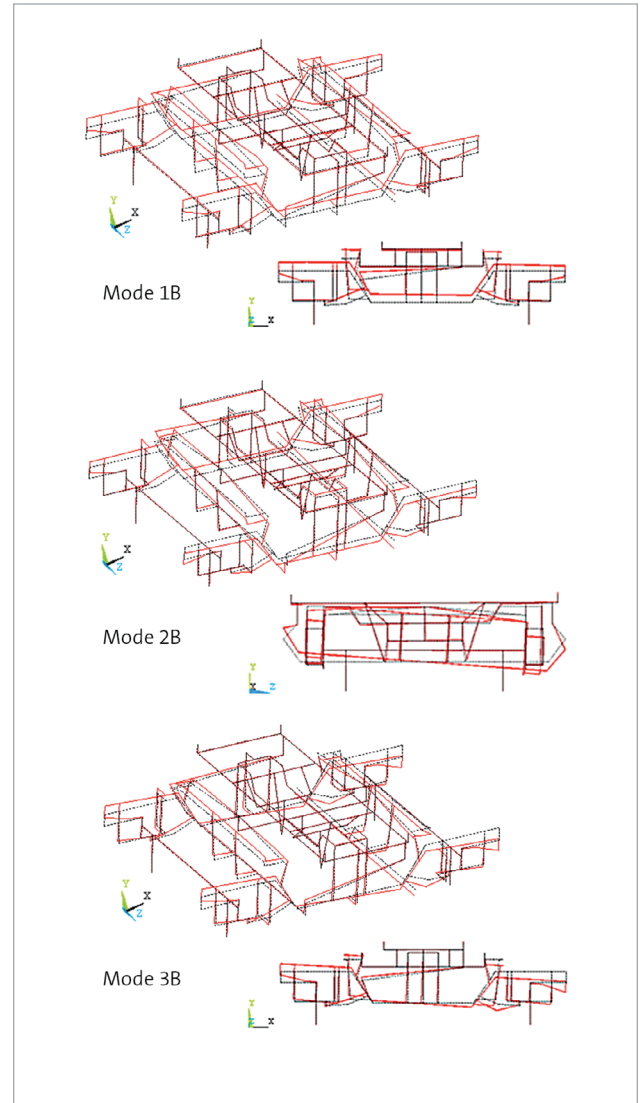


Figure 5: Numerical modes of vibration of the bogies.

where  $f_i^{exp}$  and  $f_i^{num}$  are the experimental and numerical frequencies referring to mode  $i$ ,  $\varphi_i^{exp}$  and  $\varphi_i^{num}$  are the vectors containing the experimental and numerical modal information related to mode  $i$ ,  $a$  and  $b$  are weighting factors of the objective function terms and  $n$  is the total number of vibration modes.

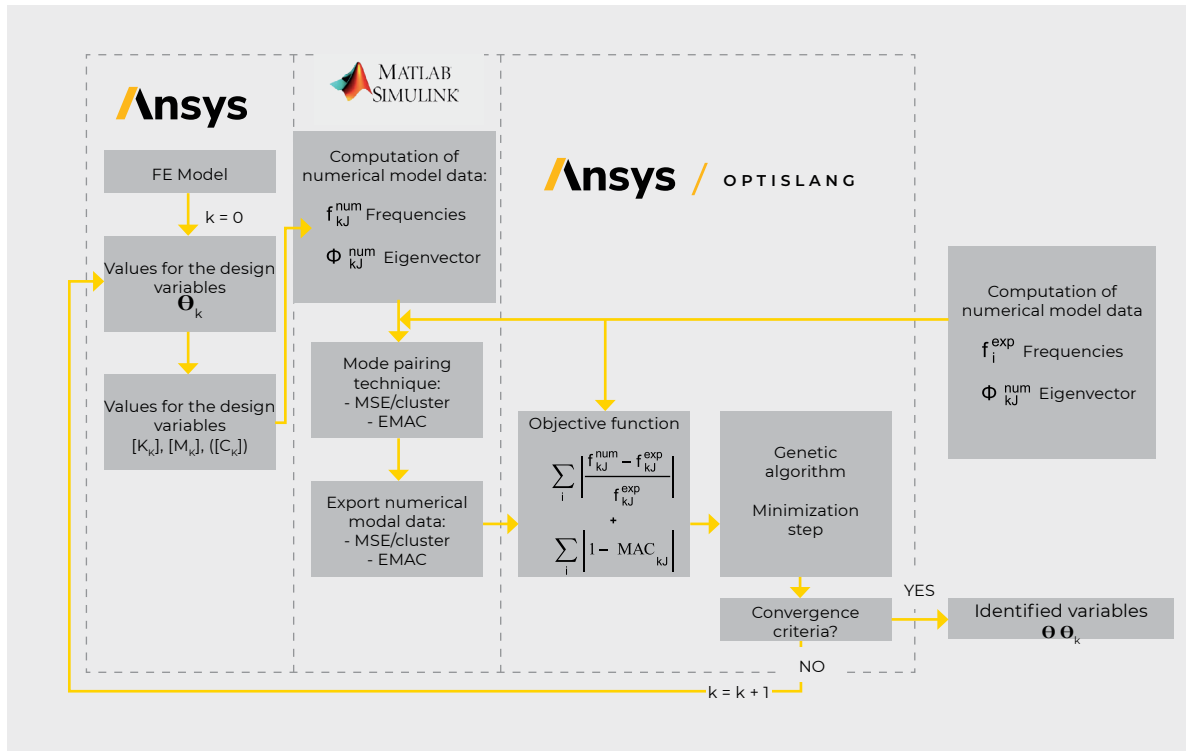


Figure 6: Calibration methodology for the numerical model.

## / Calibration

The experimental calibration of the numerical model of the BBN vehicle was performed based on modal parameters which were identified by the dynamic tests of the bogie and car body. The first phase focused on the calibration of the numerical model of the bogie under test conditions [1]. The second phase focused on the calibration of the complete numerical model of the vehicle. The numerical parameters of the bogie estimated in the first phase were assumed as deterministic parameters in the second phase.

### Calibration of the bogie

#### Numerical model under test conditions

The calibration of the numerical model of the bogie forced the development of a model that would reproduce the specific conditions of the test. Changes to the original model involved the removal of springs and dampers from the secondary suspensions and from the tilting and load bolsters. Elements were also added to simulate the interface between the bogie and the actuation system, including distribution blocks and elastic blocks of the secondary suspensions. Rigid supports were introduced, at the contact point of the hydraulic actuators, with the ability to assume different positions, thus meeting the deviations of the contact point in the longitudinal ( $x$ ) and transverse ( $z$ ) directions. The elastic blocks of the suspension were modeled by spring elements positioned in the vertical direction. The stiffness of the contact between distribution blocks and elastic blocks of the suspension was also modeled, in the  $x$  and  $z$  directions, through spring elements. Table 5 describes the mechanical and geometrical parameters of the numerical. These parameters should be considered together with the parameters indicated in Table 3.

Parameter	Designation	Type	Statistical distribution		Adopted value	Unit
			Average value/ standard deviation	Limits (lower/upper)		
$K_b$	Stiffness of the secondary suspension's elastic block Dir $y^a$	Uniform	12,000/1732	9000/15,000	12,000	kN/m
$K_{btl}$	Dir x and Dir $z^a$	Uniform	25,250/14,289	500/50,000	5000	kN/m
$Pos_{le}$	Position of the contact point of the actuation system Dir $x^a$ Left side	Uniform	5/1.7	2/8	5	-
$Pos_{ld}$	Right side					
$Pos_{te}$	Dir $z^a$ Left side	Uniform	0/0.6	-1/1	0	-
$Pos_{td}$	Right side					
$E_m$	Modulus of deformability of wood	Uniform	8/2.3	4/12	10	GPa

Table 5: Characteriation of the parameters of the numerical model of the bogie under test conditions (according to the referential of Figure 8).

The position of the contact point with the actuation system, in longitudinal and transverse directions, may assume different values for the left and right hydraulic actuators. The longitudinal position of the actuator was limited to positions 2–8.

### Sensitivity Analysis

Figure 7 shows the results of the global sensitivity analysis using Spearman's rank correlation coefficient. This sensitivity analysis was performed using a stochastic sampling technique based on 500 samples generated by the Latin Hypercube method. This analysis was based on the parameters intervals presented in Tables 3 and 5. The correlation coefficients between  $[-0.25, 0.25]$  were excluded from the graphical representation. The random generation of samples, particularly the parameters of the bogie's additional mass, was subject to the following restrictions:

$$-\varepsilon \leq \Delta M - [L_{lc} \Delta M_{lc} + L_{le} \Delta M_{le} + L_t \Delta M_t] \leq \varepsilon$$

where  $\Delta M$  equals 842 kg, and  $L_{lc}$ ,  $L_{le}$  and  $L_t$  represent the total length of the central area of the girders, the extremities of the girders and crossbars, equal to 4.46 m, 3.56 m and 5.26 m, respectively, and  $\varepsilon$  is a tolerance considered equal to 150 kg.

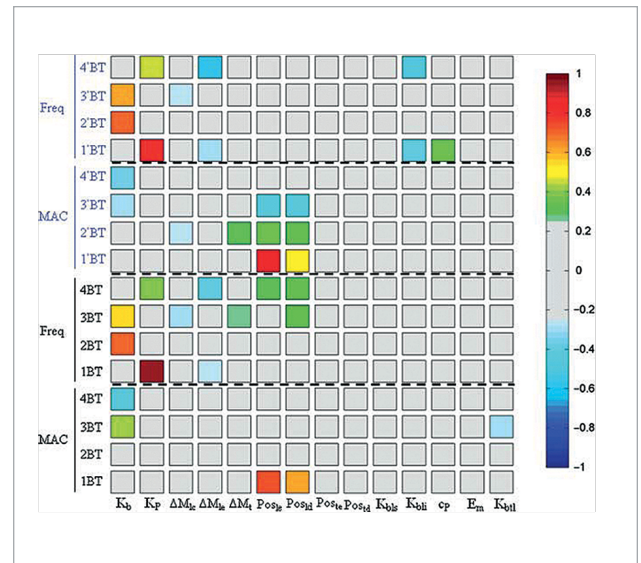


Figure 7: Spearman's rank correlation coefficient between the parameters and responses of the numerical model of the bogie under test conditions.



The correlation matrix shows that the stiffness of the primary suspensions, the additional mass of the girders (central area and extremities) and the stiffness of the lower traction rod of the axle box have significant influence over the vibration frequencies. In turn, the position of the actuators affects MAC values, particularly in modes 1BT. The vertical stiffness of the secondary suspension blocks influences the vibration frequencies and also the MAC values in a significant way. The remaining analysed parameters do not have significant influence on the modal responses and were therefore excluded from the optimization phase. The influence of the primary suspensions' stiffness over the frequencies of modes 1BT and 4BT, for which the distance between the suspensions and the rotation axle of the bogie is larger, should be emphasised. In these modes the elastic block of the suspension has no influence over the responses due to its location near the rotation axle. It is not the case of the frequencies of modes 2BT and 3BT, which involve transverse translation and rotation of the bogie, respectively, and for which the stiffness of the suspension blocks, compared with the primary suspensions, is decisive for controlling the responses.

### Optimization

The optimization of the model involved 10 numerical parameters and 16 modal results (8 vibration frequencies and 8 MAC values). The genetic algorithm was based on an initial population of 30 individuals considering 250 generations, in a total of 7500 individuals. The initial population was randomly generated by the Latin Hypercube method. A number of elites equal to 1 and a number of substitute individuals also equal to 1 have been defined in this algorithm. The crossover rate was assumed to be 50% and the mutation rate was considered equal to 15% with a standard deviation variable along the optimization between 0.10 and 0.01.

The objective function considers a total number of vibration modes equal to 8 and weighting factors a and b equal to 1. The optimization problem still includes restrictions related to the parameters of additional mass of the bogie. Optimal values of the parameters were obtained from the results of four independent optimization cases (GB1-GB4) based on different initial populations. Figure 8 shows the ratios of the values of each parameter of the model in relation to the limits indicated in Tables 1, 3 and 5. The limits of the distributions of some of the parameters were extended, such as the cases of the stiffness of the primary suspension (500/1000 kN/m), and the stiffness of the axle box's traction rods (3/10 and 10/40MN/m) due to the systematic tendency of the optimum solutions of these parameters to reach the limits indicated in Table 3. A 0% ratio means that the parameter coincides with the lower limit. A ratio of 100% means that it coincides with the upper limit. The stiffness and damping parameters of the primary suspension and increments of mass are presented in Figure 8a indicating, in brackets, the numerical parameters' values.

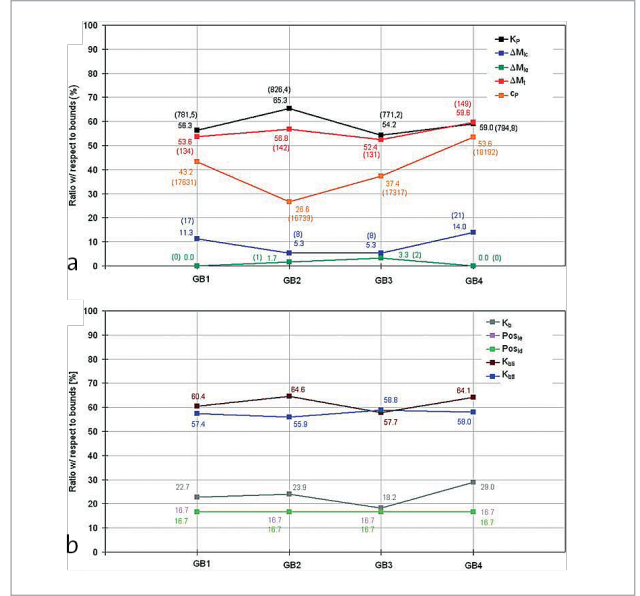


Figure 8: Values of numerical parameters for optimization cases GB1-GB4: (a) stiffness and damping of the primary suspension and increment of masses; (b) characteristics of the elastic elements and actuation system.

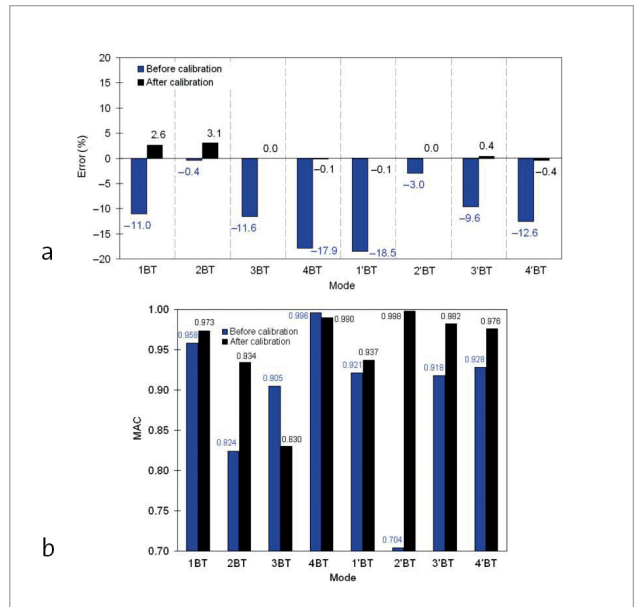


Figure 9: Comparative analysis of the errors of experimental and numerical responses, before and after calibration: (a) vibration frequencies; (b) MAC.

The parameters related to the elastic elements (blocks and rod) and actuation system is shown in Figure 8b. The analysed parameters present a good stability with variations below 10%, except for the damping of the primary damper. This is one of the parameters that the sensitivity analysis has shown to have a smaller influence over the numerical responses. Figure 9 summarises the error values between the numerical and experimental vibration frequencies, taking as reference the average values of the experimental frequencies, and the values of the MAC parameter, before and after calibration. The results after calibration are related to optimization case GB2, which was the one presenting the lowest residual of the objective function. The average error of the frequencies decreased from 10.6% before calibration to 0.8% after calibration. In turn, the average value of the MAC parameter increased from 0.894 before calibration to 0.953 after calibration. As visualised in Figure 10, the experimentally obtained and numerically derived optimised modal configurations of the bogie coincide almost perfectly.

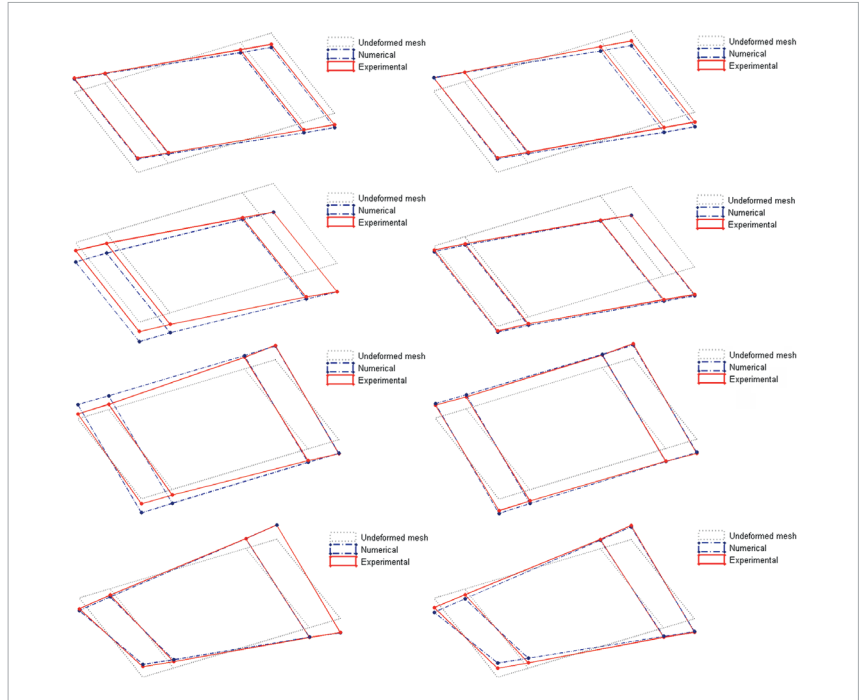


Figure 10: Comparison between the experimental and numerical vibration modes of the bogie after calibration.

## Calibration

### Sensitivity analysis

Figure 11 presents the results of the global sensitivity analysis using Spearman's rank correlation coefficient. The sensitivity analysis was performed using a stochastic sampling technique based on 250 samples generated by the Latin Hypercube method. This analysis was based on the parameters intervals presented in Table 2. The random generation of samples, particularly for the parameters of the car body's additional mass, was subject to the following restrictions:

$$-\varepsilon \leq \Delta M - [L_{lc}\Delta M_{lc} + L_{le}\Delta M_{le} + L_t\Delta M_t] \leq \varepsilon$$

where  $\Delta M$  and  $L_t$  represent the additional mass on the base, side walls and cover, respectively, and  $\varepsilon$  is a tolerance equal to 10%. The mode pairing was performed by application of a technique based on the modal strain energy and on the EMAC parameter. The correlation matrix shows that the stiffness of secondary suspensions, from front (KS1) and rear (KS2) bogies, has significant influence over the frequencies and MAC values of the rigid body modes of the car body. In turn, the RMI parameters from the base (RMIb) and side walls (RMIp) essentially control the frequencies and MAC values of the structural modes of the car body. The parameters additional mass and stiffness of the connecting rod between the tilting and load bolsters (Kb) have significant influence over the vibration frequency of mode 1C. The remaining analysed parameters did not have significant influence with respect to the modal responses, and were consequently excluded from the optimization phase. It is possible to verify that the flexural stiffness of the side walls, which is controlled by the walls' RMI parameter, is important for controlling the torsional stiffness of the car body, as demonstrated by the high value of the correlation coefficient between the walls RMI parameter and the frequency of mode 4C.

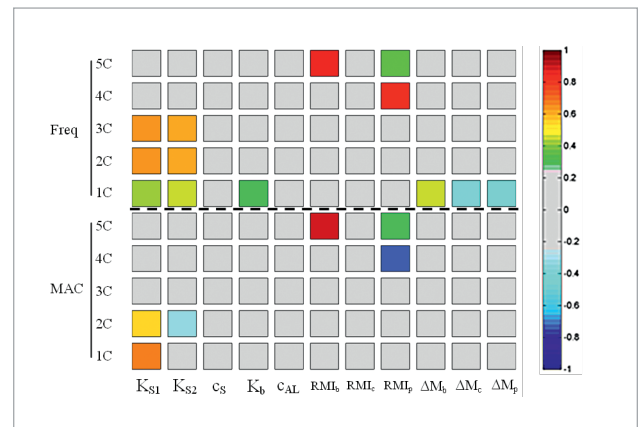


Figure 11: Spearman's rank correlation coefficient between the parameters and responses of the carbody's numerical model.

## Optimization

The optimization of the model finally involved 7 numerical parameters and 10 modal results (5 vibration frequencies and 5 MAC values). The control parameters of the genetic algorithm and the objective function are identical to those in the optimization of the bogie. The optimization problem also included constraints involving the car body's additional mass parameters. Optimal values of the parameters were obtained from the results of four independent optimization cases (GC1–GC4) based on different initial populations. Figure 12 (see page 28) shows the values' ratios of each parameter of the model in relation to the limits given in Table 1. The lower and upper stiffness limits of the secondary suspension were extended from 242 and 272.9 kN/m to 200 and 400 kN/m, respectively. Parameters related to the characteristics of the secondary suspension, connecting rod and geometrical properties of the car body are presented in Figure 12a indicating, in brackets, the estimated values for the stiffness of the secondary suspension. The parameters referring to mass distribution are presented in Figure 12b.

It is noticeable that the most stable parameters, with variations below 10%, are those that most affect the responses, including the stiffness of secondary suspensions and RMI parameters of the base and side walls. The stiffness values of the front bogie's secondary suspension are higher than those estimated for the rear bogie. Regarding the additional masses of the side walls and cover, the estimates show higher variations, close to 25%. This should be related to the fact that these parameters contribute in a similar way to the participant mass on vibration mode 1C. Therefore, there may be different combinations of these parameters leading to the same solution, in terms of optimization of the problem. Figure 13 summarises the error values of the numerical and experimental vibration frequencies taking as reference the average values of the experimental frequencies, and of the MAC parameter, before and after calibration. The results after calibration are related to the GC1 optimization case, which was the one with the lowest final residual of the objective function. The frequencies' average error dropped from 20.3%, before calibration, to 2.9%, after calibration. This error decrease is mainly due to the reduction of the error associated with the frequencies of structural modes 4C and 5C. The average value of the MAC parameter did not change significantly, increasing from 0.927, before calibration, to 0.937, after calibration. The excellent agreement between the car body's experimentally obtained and numerically derived optimised modal configurations can be verified in Figure 14.

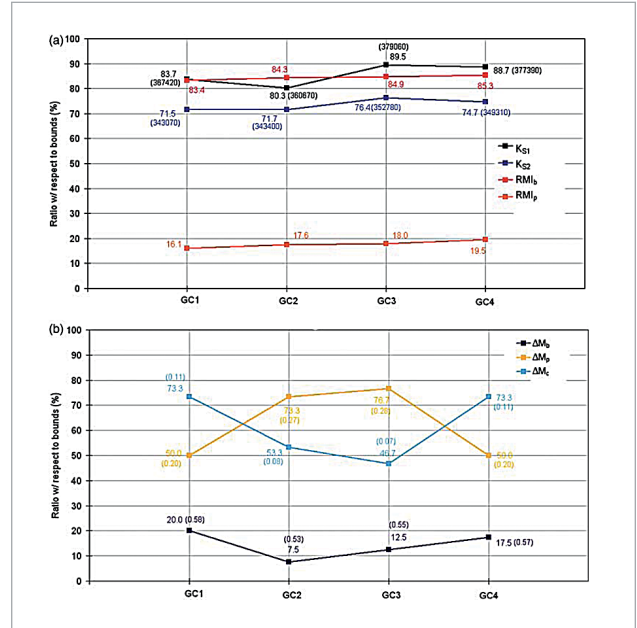


Figure 12: Values of numerical parameters for optimization cases GC1–GC4: (a) characteristics of the suspension, connecting rods and geometrical properties of the carbody; (b) masses

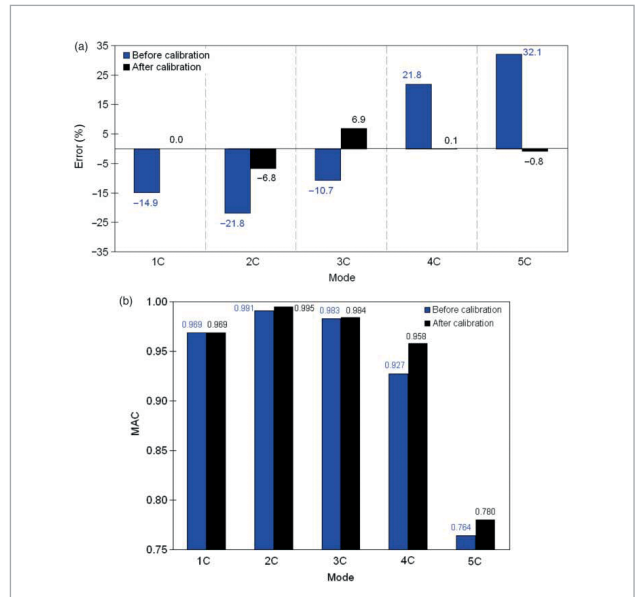


Figure 13: Comparative analysis of the errors from the experimental and numerical responses, before and after calibration in terms of: (a) vibration frequencies; (b) MAC.

## Final Results

The combination between the numerical parameters, obtained for the optimization case of the bogie GB2, and the parameters obtained in optimization case of the complete vehicle GC1, were the basis for the establishment of the vehicle's calibrated numerical model. Table 7 presents the values of the damped vibration frequencies of the main vibration modes of the BBN vehicle obtained from the calibrated numerical model. Comparing the values of the frequencies with the values given in Table 4, concerning the initial numerical model, there is a visible tendency towards the frequency increase on the rigid body modes of the car body and bogies, being that, in the bogies' case, this increase ranged from 10% to 55%. This tendency is due to the significant increase of the stiffness of the primary and secondary suspension springs. In turn, the structural modes of the car body, particularly modes 4C and 5C showed a decreased tendency of approximately 20%, mainly due to the reduction of the RMI parameter of the car body's side walls.

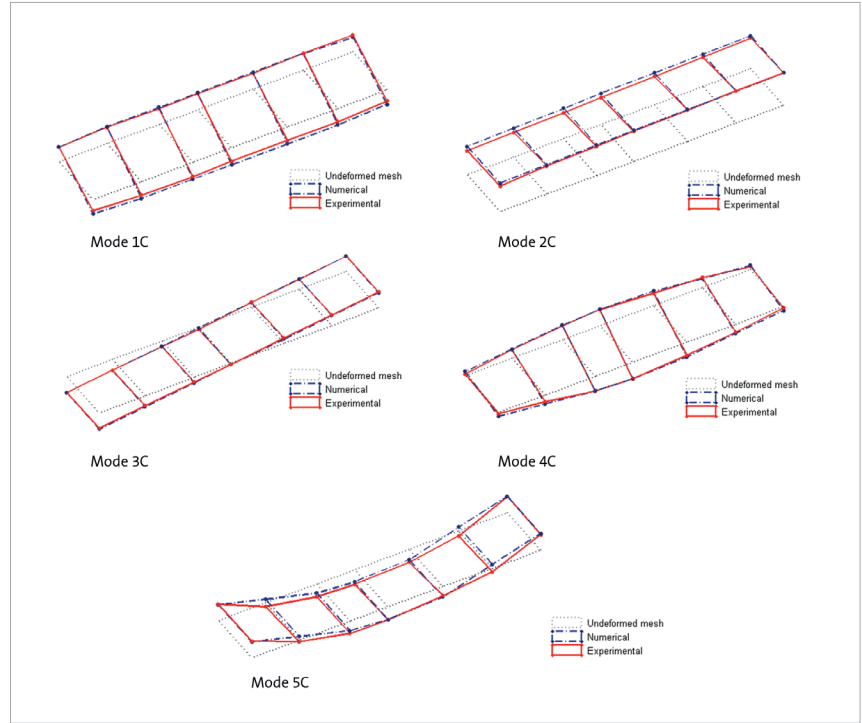


Figure 14: Comparison between the vibration modes of the carbody, experimentally and numerically obtained, after calibration.

## Conclusion

This article described the calibration of the numerical model of a BBN vehicle of the Alfa Pendular train based on modal parameters. The calibration of the numerical model was conducted through an iterative methodology based on an optimization algorithm and was performed using a multistep approach involving two phases: the first phase focused on the calibration of the model of the bogie under test conditions and the second focused on the calibration of the complete model of the vehicle. Global sensitivity analysis allowed the identification of numerical parameters to be considered in the calibration. The parameters that have shown the highest sensitivities in relation to the modal responses were, for the bogie, the vertical stiffness of the secondary suspension block and the vertical stiffness of the primary suspensions. As for the car body, the RMI parameters of the base and side walls and the vertical stiffness of the secondary suspension were the parameters with highest sensitivity in relation to the modal responses.

Element	Mode	Damped frequency (Hz)
Carbody	1C	1.01
	2C	1.24
	3C	1.70
	4C	8.39
	5C	12.16
Bogies	1B	9.21/9.24
	2B	7.70/8.12
	3B	14.16/14.09

Table 7: Natural frequencies of the BBN vehicle obtained from the calibrated numerical model.

The optimization was conducted using a genetic algorithm involving a total of 17 numerical parameters and 26 modal responses. The results of the optimization cases of the bogie and vehicle, based on different initial populations, led mostly to very stable numerical parameters' values, particularly for those highly correlated with the responses. The comparison between the numerical vibration frequencies' values, before and after calibration, and the experimental vibration frequencies, has revealed significant improvements on the initial numerical models. The average error of vibration frequencies of the modes of the bogie under test conditions went from 10.6%, before calibration, to 0.8%, after calibration. Concerning the vibration modes of the complete model of the vehicle, the average error of frequencies went from 20.3%, before calibration, to 2.9% after calibration. Significant improvements were also observed in MAC values, particularly in the vibration modes of the bogie. This result demonstrates the robustness and efficiency of genetic algorithms on the estimation of the vehicle's modal responses. The combination of numerical parameters obtained for the GB2 bogie optimization case with the parameters obtained for the GC1 case of vehicle optimization provided the basis for developing the calibrated numerical model of BBN vehicle. Compared with the initial numerical model, the calibrated numerical models show higher frequency values of the rigid body modes of the car body and bogies, essentially due to the increased stiffness of the primary and secondary suspension springs. On the other hand, most of the car body's structural modes tended to decrease, largely due to a reduction of the RMI parameter of the side walls of the vehicle's car body. In future studies, the calibrated numerical model of the vehicle will be used to access the dynamic behaviour of the train-track coupled system, in terms of passengers comfort and wheel-rail contact stability, on plain track, on bridges or on transition zones.

### **/ Authors**

D. Ribeiro (School of Engineering, Polytechnic of Porto) / R. Calçada, R. Delgado ( Faculty of Engineering, University of Porto) / M. Brehm (BATir – Structural and Material Computational Mechanics, Université Libre de Bruxelles) / V. Zabel (Bauhaus-University Weimar)

### **/ References**

[1] D. Ribeiro, R. Calçada, R. Delgado, M. Brehm and V. Zabel (2013) - "Finite element model updating of a railway vehicle based on experimental modal parameters", *Vehicle System Dynamics*, 51 (6), pp. 821-856.

**ANSYS, Inc.**  
Southpointe  
2600 Ansys Drive  
Canonsburg, PA 15317  
U.S.A.  
724.746.3304  
ansysinfo@ansys.com

If you've ever seen a rocket launch, flown on an airplane, driven a car, used a computer, touched a mobile device, crossed a bridge or put on wearable technology, chances are you've used a product where Ansys software played a critical role in its creation. Ansys is the global leader in engineering simulation. We help the world's most innovative companies deliver radically better products to their customers. By offering the best and broadest portfolio of engineering simulation software, we help them solve the most complex design challenges and engineer products limited only by imagination.

**Visit [www.ansys.com](http://www.ansys.com) for more information.**

Any and all ANSYS, Inc. brand, product, service and feature names, logos and slogans are registered trademarks or trademarks of ANSYS, Inc. or its subsidiaries in the United States or other countries. All other brand, product, service and feature names or trademarks are the property of their respective owners.

© 2020 ANSYS, Inc. All Rights Reserved.